Biophysical Journal Volume 79 July 2000 14–25

Quinone-Dependent Delayed Fluorescence from the Reaction Center of Photosynthetic Bacteria

Kinga Turzó, Gábor Laczkó, Zoltán Filus, and Péter Maróti*
Department of Biophysics, University of Szeged, Szeged H-6722, Hungary

ABSTRACT Millisecond delayed fluorescence from the isolated reaction center of photosynthetic bacteria *Rhodobacter sphaeroides* was measured after single saturating flash excitation and was explained by thermal repopulation of the excited bacteriochlorophyll dimer from lower lying charge separated states. Three exponential components (fastest, fast, and slow) were found with lifetimes of 1.5, 102, and 865 ms and quantum yields of 6.4×10^{-9}, 2.2×10^{-9}, and 2.6×10^{-9} (pH 8.0), respectively. While the two latter phases could be related to transient absorption changes, the fastest one could not. The fastest component, dominating when the primary quinone was prereduced, might be due to a small fraction of long-lived triplet states of the radical pair and/or the dimer. The fast phase observed in the absence of the secondary quinone, was sensitive to pH, temperature, and the chemical nature of the primary quinone. The standard free energy of the primary stable charge pair relative to that of the excited dimer was -910 ± 20 meV at pH 8 and with native ubiquinone, and it showed characteristic changes upon pH and quinone replacement. The interaction energy (~50 meV) between the cluster of the protonatable groups around GluL212 and the primary semiquinone provides evidence for functional linkage between the two quinone binding pockets. An empirical relationship was found between the *in situ* free energy of the primary quinone and the rate of charge recombination, with practical importance in the estimation of the free energy levels from the easily available lifetime of the charge recombination. The ratio of the slow and fast components could be used to determine the pH dependence of the free energy level of the secondary stable charge pair relative to that of the excited dimer.

INTRODUCTION

The reaction center (RC) is a membrane-bound pigment-protein complex of the purple nonsulfur photosynthetic bacteria *Rhodobacter (Rb.) sphaeroides* that performs the initial steps of conversion of light energy to chemical energy (Cramer and Knaff, 1990; Okamura and Feher, 1995). After absorption of a photon, the bacteriochlorophyll dimer (P) is promoted to the excited singlet state (P*). A particular feature of the excited dimer of the RC is the capacity to perform charge separation by transferring an electron from P* to the closest-lying cofactor, a bacteriochlorophyll monomer within 3 ps. The initial electron transfer (ET) is followed by an even faster (0.9 ps) step to a bacteriopheophytin (I) before it proceeds in 200 ps to the primary quinone (Q_A) and in 3–200 μs to the secondary quinone (Q_B), as revealed by the characteristic spectral transients (Martin et al., 1986; Fleming et al., 1988; Arlt et al., 1993; Li et al., 1998). The ET in photosynthetic RC is unique among electron transfer reactions in biological systems, as the charge separation is extraordinarily fast and retains a significant fraction of the original photon energy with a quantum yield very close to 100% (*i.e.,* every photon absorbed by the dimer evokes a productive ET; Wraight and Clayton, 1973). The high quantum yield arises from the rapid stabilization of the ET states, which are progressively more stable. The final $P^+Q_B^-$ charge-separated state has a lifetime as large as 1 s at neutral pH. The price for this high specificity and stability of the ET is a relatively large free energy loss in the process: the final $P^+Q_B^-$ state conserves only about one-third of the 1.38-eV photon energy in the form of standard free energy relative to its ground state (PQ_B). During the subsequent electron transfer processes, an electron donor (ferrocytochrome c_2) will donate an electron to P^+ and the dimer will be prepared again for a new charge separation. If, however, no exogenous donor to P^+ is available, then the electron on the series of acceptors would recombine with P^+.

The two acceptor quinones are chemically identical in many bacterial species (ubiquinone-10 in *Rb. sphaeroides*) but are modified by the protein environment to play radically different roles in the reaction cycle of the RC (McComb et al., 1990; Wraight, 1998). The primary quinone is tightly bound into a relatively hydrophobic part of the M subunit, it makes one-electron chemistry, and operates between the neutral quinone (Q_A) and the anionic semiquinone (Q_A^-) forms. In contrast, the secondary quinone is reversibly bound in a more polar region of the L subunit, it is a two-electron acceptor, and all of its three redox forms (quinone, semiquinone (Q_B^-), and quinol (Q_BH_2)) participate in the turnover of the RC: the doubly reduced quinone dissociates from the RC and is replaced by a quinone from the pool of quinones (Okamura and Feher, 1995; Osváth and Maróti, 1997). The significant functional differences between the two quinones or between the native and substituted quinones at the Q_A binding site can be attributed largely to the differences in the standard free energy levels ($G°$) of the quinones.

Received for publication 6 December 1999 and in final form 5 April 2000.
Address reprint requests to Dr. Peter Maróti, Department of Biophysics, Jozsef Attila University Szeged, Egyetem Utca 2, Szeged H-6722, Hungary. Tel.: 36-62-544-120; Fax: 36-62-544-121; E-mail: pmaroti@physx.u-szeged.hu.

0006-3495/00/07/14/12 $2.00

The $G°$ values relative to that of an upper lying state can be estimated by tracking 1) the indirect means of charge recombination and 2) the delayed fluorescence emission of the dimer.

1) The charge recombination from the $P^+Q_A^-$ state can follow two routes, and the rate of the observed reaction will be the sum of the rates of the two reactions (Feher et al., 1988). The first reaction is a direct tunneling to the ground state, and the second one is an uphill (indirect) reaction to P^+I^-, where $P^+Q_A^-$ preequilibrates with P^+I^- before decaying to the ground state. The free energy level of the $P^+Q_A^-$ state relative to that of the P^+I^- state can be determined from the relative contribution of the uphill reaction. The charge recombination reaction has been used as an *in situ* monitor of the $P^+Q_A^-$ free energy by several groups (Gunner et al., 1986; Gunner and Dutton, 1989; McComb et al., 1990; Schelvis et al., 1992). The back-reaction from $P^+Q_B^-$ occurs predominantly via Q_A^- in wild-type RC; therefore G_B° relative to G_A° can be calculated from the observed charge recombination rates k_{AP} and k_{BP} (Wraight and Stein, 1983; Kleinfeld et al., 1984).

2) The origin of the delayed fluorescence from the dimer is the thermal repopulation of P* from any of the charge-separated P^+Q^- states via reversed electron transfer (for a review of the earlier results see Fleischman, 1978). The kinetics of delayed fluorescence follows the kinetics of the charge recombination. The free energy levels of the quinone states relative to that of the excited dimer can be determined from the ratio of the amplitudes (or intensities) of the delayed and prompt fluorescence (Arata and Parson, 1981; Turzó et al., 1999). Because of the very low intensity and the near-infrared emission, the measurement of delayed fluorescence in the millisecond time domain (contrary to that in the pico- and nanosecond range; see Ogrodnik et al., 1999, for a recent review) has not become a routine method of free energy determination (Woodbury et al., 1986). It has the great advantage, however, of providing the free energy levels relative to that of the excited dimer, which is considered fairly stable upon slight modification of the structure and environment of the cytoplasmic side of the RC. The delayed fluorescence technique for a series of quinone-substituted RCs was used by Woodbury et al. (1986) to establish a relationship between the free energy of the $P^+Q_A^-$ state and the rate constant of the decay from this state. This has notable practical importance, as the rate of charge recombination is more readily available than the free energy level determined from delayed fluorescence (Schmid and Labahn, 1998; Schmid et al., 1999). This topic was elaborated in more detail and quantified by Gunner and Dutton (1989) in terms of a linear relationship between the logarithm of the rate constant for the decay of $P^+Q_A^-$ via the intermediate P^+I^- state and the standard free energy of $P^+Q_A^-$.

The current work is aimed at measuring the decay of the delayed fluorescence in the millisecond time range, where the states of the acceptor quinones have a major impact on the kinetics. The origin and the properties of the observed three components will be discussed in terms of model calculations, the structure and function of the RC. By comparison of the intensities of the prompt and delayed fluorescence, the free energy levels of the charge-separated P^+Q^- states relative to that of the excited dimer will be determined under different conditions like pH and substitution of the native primary quinone with different benzoquinones and naphthoquinones. Based on the measurement of the free energy states of several high-potential quinones at the Q_A binding pocket and the corresponding rates of direct recombination, a calibration line is constructed that would be useful for estimation of the free energy level of a substituted quinone from the (easily) observable rate of charge recombination. The free energy differences between P* and $P^+Q_B^-$, determined by two different (kinetic and delayed fluorescence) methods, will be compared.

MATERIALS AND METHODS

The carotenoidless mutants (R26) of the nonsulfur purple bacteria *Rhodobacter sphaeroides* were grown for 3–5 days under anaerobic conditions in a luminostat at a temperature of ~30°C. The RCs from bacterial cells were isolated with the ionic detergent *N,N*-dimethyldodecyl-amine-*N*-oxide (LDAO), followed by purification using ammonium sulfate and diethylaminoethyl chromatography (Maróti and Wraight, 1988). The ratio of the optical densities at 280 nm and 802 nm (OD_{280}/OD_{802}, defined as purity of the sample) was less than 1.30 for all preparations. The RC concentration was determined from the steady-state optical densities at 802 nm or 865 nm, using extinction coefficients of $\varepsilon_{802} = 0.288\ \mu M^{-1}\ cm^{-1}$ or $\varepsilon_{865} = 0.135\ \mu M^{-1}cm^{-1}$. The ionic detergent LDAO was removed and replaced by a nonionic detergent Triton X-100 after a long (48 h) dialysis at 4°C by a frequent change of the dialyzing medium. The pH was measured with a combined glass electrode (model 91-03; Orion) calibrated with standards that spanned the measured pH range. The assay solution contained 2 μM RCs with 0.03% Triton X-100, 100 mM NaCl, and 5 mM buffer, depending on the pH.

Q_A and Q_B were removed by high concentrations of LDAO (4.5%) and orthophenantroline (10 mM) by the method of Okamura et al. (1975), with minor modifications by Liu et al. (1991). The procedure typically yielded RCs with no secondary quinone activity and ~5% primary quinone activity, as measured by the rate and amplitude of flash-induced charge recombination observed at 430 nm (Kleinfeld et al., 1984; Maróti and Wraight, 1988). The quinone activities were reconstituted by the addition of (native or artificial) quinones in excess to the RC solution and incubated for several hours with stirring at 4°C. DQ was solubilized in ethanol, MD was solubilized in water, and the long-tailed UQ_{10} was dissolved and homogenized in Triton X-100 before use (McComb et al., 1990). The delayed fluorescence of various samples was compared, and only a minor influence of the RC preparation and quinone substitution was found.

The kinetics of the ms delayed fluorescence of the RC after single flash excitation was measured with a homemade fluorometer (Fig. 1). The major difficulties arose from the extremely low yield of delayed fluorescence (in the range of 10^{-9}), the near-IR emission wavelength (the maximum of fluorescence is centered at 920 nm; Osváth et al., 1996), and the intense prompt fluorescence emitted during excitation. The RC was excited by a frequency-doubled and Q-switched Nd:YAG laser flash (Quantel YG 781-10, wavelength 532 nm, energy 100 mJ, duration 5 ns). The laser beam was introduced into a light-tight box through a green filter (Schott BG-18). The sample was in a thermostatted 1-cm rectangular quartz cuvette selected for

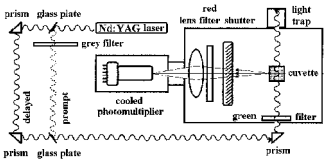

FIGURE 1 An optical arrangement for measuring the millisecond delayed fluorescence of the reaction center protein of photosynthetic bacteria. The intensity of the laser light used for the excitation of prompt fluorescence is attenuated by inserting low-reflection glass plates and neutral density filters in the light path (the transmitted light is blocked). See the text for more details.

extremely low fluorescence ("far UV"; Thermal Syndicate). The fluorescence of the RC was focused through an IR cutoff filter (Schott RG-850) onto the photocathode of a red-sensitive photomultiplier (Hamamatsu R-3310-03). The electronically controlled mechanical shutter (Uniblitz VS25) protected the photomultiplier from the very intense prompt fluorescence (the opening time of the shutter was 3 ms). The signal-to-noise ratio of the delayed fluorescence was increased by cooling the photomultiplier down to −30°C (Photocool PC 410CE; Products for Research) and by averaging. Under our conditions, the individual traces of the delayed fluorescence could be averaged at a repetition rate of 1 Hz (for RCs without secondary quinone activity) and 0.24 Hz (for Q_B-reconstituted RCs). Two hundred fifty-six decays were averaged with a digital oscilloscope (Philips PM 3350A), then stored and analyzed in a PC. The kinetic traces of the delayed fluorescence were decomposed into the sum of exponential functions, using nonlinear least-square fitting.

The integrated intensities of prompt and delayed fluorescence from the RCs were measured and compared under exactly the same optical and electrical conditions, except for the excitation energies (Arata and Parson, 1981): 0.77 mJ ± 5% laser energy was used to excite the delayed fluorescence (this energy falls in the linear range of the saturation curve; data not shown) but was attenuated to 16.2 nJ ± 10% to excite the prompt fluorescence. The energy of the laser flash was measured with a calibrated pyroelectric joulemeter (Molectron J25).

THEORY

The delayed fluorescence from bacterial RC is emitted by the excited dimer (P*). This fluorescence has a photochemical origin, resulting from the back-reaction of the primary photoproducts, and is of the leakage type. The discrimination between prompt and delayed emission and the kinetics of delayed light after flash excitation can be treated exactly in a system in which part of the energy of the excited pigment can be transiently stored in a single charge-separated state P^+Q^-. The results for this simple case are generalized and utilized in a more complex system with several transient states like the bacterial RC.

Fluorescence from a system with two transient states

Fluorescence is generated from the electronically excited state of the pigment (P*) by return to the ground state (P) with ejection of a photon (Fig. 2; now $k_+ = k_- = k_Q = 0$). The intensity of fluorescence at any time *(t)* is proportional

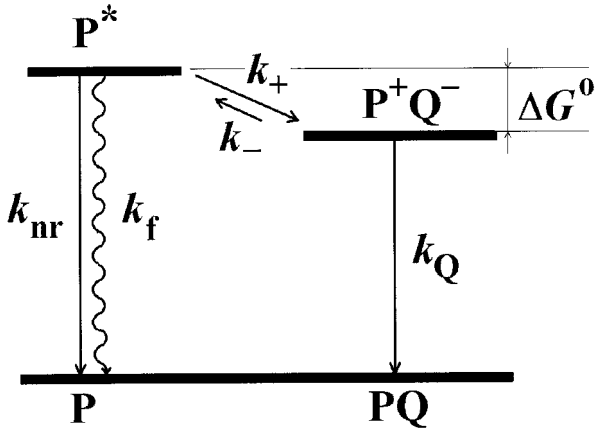

FIGURE 2 A simplified model for the determination of the decay law of fluorescence and separation of prompt and delayed fluorescence after single-flash excitation. The model includes two transient states: the singlet excited state of the pigment (P*) and the charge-separated state (P^+Q^-). Q is a general term for an electron acceptor, k_Q is the rate constant for the recombination, and $\Delta G°$ is the free energy gap between P* and P^+Q^-.

to the concentration of the excited pigment:

$$F(t) = k_f \cdot [P^*](t) \tag{1}$$

where k_f is the rate constant of fluorescence emission. This process goes on parallel to the competing radiationless transition (rate constant k_{nr}). The observed rate constant of deactivation of P* is

$$k_P = k_f + k_{nr} \tag{2}$$

After excitation of P, the time dependence of the concentration of P* is described by

$$\frac{d[P^*]}{dt} = -k_P \cdot [P^*] \tag{3}$$

with a solution of

$$[P^*](t) = \exp(-k_P \cdot t) \tag{4}$$

if the concentration of the excited pigment is taken to be unity at $t = 0$. Thus the observed decay of fluorescence of a free pigment is monoexponential, the rate constant is the sum of the rate constants of the radiative and radiationless transitions, and the yield of fluorescence is

$$\eta_0 = \frac{k_f}{k_P} \tag{5}$$

In contrast to the free pigment, the fluorescence properties of a pigment coupled to a photochemical process will be quite different (Fig. 2; $k_+ \neq 0$). The excitation energy of the pigment can be trapped by photochemical states (*e.g.,* triplet states, charge-separated states, etc.), and therefore it is lost with respect to fluorescence. The capture of the excitation energy can be irreversible or reversible.

If the trapping (rate constant k_+) is irreversible ($k_- = 0$), then the expressions derived for a free pigment (Eqs. 3–5) can be extended accordingly. After instant excitation, the decay of the concentration of the excited pigment is

$$[P^*](t) = \exp(-(k_P + k_+)\cdot t) \tag{6}$$

i.e., the observed decay of fluorescence remains monoexponential but becomes faster ($k_{obs} = k_P + k_+$), and the yield

$$\eta_{prompt} = \frac{k_f}{k_P + k_+} \tag{7}$$

decreases ($\eta_{prompt} < \eta_0$).

Major alterations in the properties of fluorescence can be expected, however, if the coupling is reversible, i.e., part of the transiently stored energy can be recaptured in the form of the excited pigment. Inclusion of the back-reaction ($k_- \neq 0$) will lead to the following system of two differential equations after the flash excitation:

$$\frac{d[P^*]}{dt} = -(k_P + k_+)\cdot[P^*] + k_-\cdot[P^+Q^-] \tag{8}$$

$$\frac{d[P^+Q^-]}{dt} = k_+\cdot[P^*] - (k_Q + k_-)\cdot[P^+Q^-] \tag{9}$$

where k_- is the rate constant of the back-reaction and k_Q is the rate constant of the charge recombination, whereby the charge-separated state P^+Q^- returns to the ground state PQ. The basic feature of this system of equations is that it contains a linear expression of the rates in terms of the concentrations, which in this particular case involves two species. The general solution for the time dependence of each concentration is the sum of two exponential terms. For [P*],

$$[P^*](t) = A_1\cdot\exp(-k_1\cdot t) + A_2\cdot\exp(-k_2\cdot t) \tag{10}$$

where A_1, A_2 and k_1, k_2 are the amplitudes and the rate constants of the two components, respectively. If k_+ is much larger than the other rate constants, then the approximate solutions for the rate constants are

$$k_1 = k_+ + k_- + k_P \tag{11}$$

$$k_2 = k_Q + k_P\cdot\frac{k_-}{k_+} \tag{12}$$

and those for the amplitudes (from the initial conditions $[P^*] = 1$ and $[P^+Q^-] = 0$ at $t = 0$) are

$$A_1 = 1 - \frac{k_-}{k_+} \tag{13}$$

$$A_2 = \frac{k_-}{k_+} \tag{14}$$

The back-reaction made the decay biexponential. The rate constant of the fast phase (k_1) involves the rate of establishment of the kinetic equilibrium of the excited state (P*). Here the dominant rate constant is that of the forward reaction. This component is frequently called prompt fluorescence. The rate constant of the slower phase (k_2) reflects the rate of evacuation of the transient, free energy storage state (P^+Q^-). This process can occur through two parallel paths: direct charge recombination (rate constant k_Q) and indirectly via P* (rate constant $k_P\cdot k_-/k_+$). The slow phase is the delayed fluorescence.

The ratio of the rate constants for backward and forward reactions can be expressed by the free energy gap ΔG° between the P^+Q^- and P* states:

$$\frac{k_-}{k_+} = \exp\left(-\frac{\Delta G^\circ}{k_B T}\right) \tag{15}$$

where k_B is Boltzmann's constant and T is the absolute temperature. If $k_- \ll k_+$ (*i.e.,* $\Delta G \gg 25$ meV) then the amplitude of the prompt fluorescence is constant (close to unity). According to Eqs. 14 and 15, the amplitude of the delayed fluorescence is a very sensitive monitor of the free energy of P^+Q^- relative to that of P*: one order-of-magnitude drop/increase in the amplitude corresponds to a 58-meV increase/drop in the free energy gap at room temperature.

It is more convenient to determine the free energy gap by measuring the ratio of the intensities (instead of the amplitudes) of the prompt and delayed fluorescence. As the yield is proportional to the area under the corresponding exponential decay, the relative yield, *i.e.,* the ratio of the number of emitted photons, is

$$\frac{I_{prompt}}{I_{delay}} = \frac{A_1}{A_2}\cdot\frac{k_2}{k_1} \tag{16}$$

Using Eqs. 11–14 and replacing k_+ with k_f/η_{prompt} (see Eq. 7, which is also valid in the present approximation), we get

$$\frac{I_{prompt}}{I_{delay}} = \frac{k_Q\cdot\eta_{prompt}}{k_f}\cdot\exp\left(\frac{\Delta G^\circ}{k_B T}\right) \tag{17}$$

While the ratio of the amplitudes ($\exp(\Delta G^\circ/k_B T)$ can be extremely large, the ratio of the intensities is significantly reduced by the appearance of the ratio of the rate constants, and thus the latter quantity can be measured much easier. Taking $\Delta G^\circ = 900$ meV (Arata and Parson, 1981; Turzó et al., 1998), $k_Q = 10\ s^{-1}$, $k_f = 8\times10^7\ s^{-1}$ (Arata and Parson, 1981; McPherson et al., 1990), and $\eta_{prompt} = 4\times10^{-4}$ (Zankel et al., 1968; Woodbury et al., 1985) in bacterial RC, the ratio of the amplitudes of the prompt and delayed fluorescence amounts to 4.3×10^{15}, but that of the intensities is only 2.1×10^5.

Millisecond delayed fluorescence from the acceptor quinone system of bacterial RC

When two or more consecutive reactions are added to our simple model, the exact solution becomes very complicated. One may find an approximate solution, however, if the lifetimes of the prompt and delayed fluorescence are very different, as in the case of the millisecond delayed fluorescence from bacterial RC. Consider three steps (involving the bacteriopheophytin and the two quinones) in the process of charge stabilization in RC from *Rb. sphaeroides* (Fig. 3). In RC from wild type, the direct recombination from the $P^+Q_B^-$ state is negligible compared to the indirect decay via $P^+Q_A^-$ (Labahn et al., 1994). A system of four coupled linear differential equations (rate equations) can be set for the four transient states (P*, P^+I^-, $P^+Q_A^-$, and $P^+Q_B^-$). The general solution in thermal equilibrium can be expressed by the sum of four exponential terms. In the millisecond time range and afterward (for $t \gg 1/(k_{AB} + k_{BA})$), the slowest component will dominate and the time and free energy dependence of the delayed fluorescence from RCs with fully reconstituted Q_B activity of concentration $[RC]_B$ can be given by

$$F_B(t) = k_f \cdot [RC]_B \cdot \frac{\exp(G_B^\circ/k_BT)}{1 + \exp((G_B^\circ - G_A^\circ)/k_BT)} \cdot \exp\left(- k_A \frac{k_{BA}}{k_{AB} + k_{BA}} \cdot t \right) \quad (18)$$

Similarly, for RCs with no Q_B (only Q_A) activity,

$$F_A(t) = k_f \cdot [RC]_A \cdot \exp\left(\frac{G_A^\circ}{k_BT}\right) \cdot \exp(- k_A \cdot t) \quad (19)$$

Based on Eq. 19, the standard enthalpy (H_A°) of the $P^+Q_A^-$ state can routinely be obtained from the slope of the standard van't Hoff plot (logarithm of the amplitude of the delayed fluorescence versus $1/T$). Considering Eq. 18, similar analysis can be made for the $P^+Q_B^-$ state if $\exp((G_B^\circ - G_A^\circ)/k_BT) \ll 1$, *i.e.,* the free energy gap between the quinones is much larger than 25 meV (at room temperature). If, however, the free energy levels of the quinones are closer (*e.g.,* in cases of higher pH, high potential quinone substitution, mutations, etc.), then a more careful analysis of the delayed light emission is required to determine the enthalpy of the secondary quinone relative to that of P*.

If the reconstitution of the Q_B activity is not complete, then biphasicity is the most notable feature of the charge recombination kinetics detectable by both flash-induced absorption change and delayed fluorescence methods. A fast phase arises from RCs without bound Q_B and a slow phase from RCs with bound Q_B during the lifetime of the flash-induced $P^+Q_A^-$ state. Introducing the relative amplitude of the slow phase of the flash-induced absorption change,

$$S_{abs} = \frac{[RC]_B}{[RC]_A + [RC]_B} \quad (20)$$

and that for the delayed fluorescence,

$$S_{delay} = \frac{F_B(t = 0)}{F_A(t = 0) + F_B(t = 0)} \quad (21)$$

and using Eqs. 18 and 19, we get

$$S_{delay} = \frac{1}{1 + (1/S_{abs} - 1) \cdot (1 + e^{(G_A^\circ - G_B^\circ)/k_BT})}. \quad (22)$$

This demonstrates that the fraction of the slow component in the decay of the delayed fluorescence is smaller than that in the absorption kinetics. Whereas in the absorption kinetics the contributions of Q_A- and Q_B-active RCs are proportional to their concentrations, in the delayed fluorescence an additional weighting by a Boltzmann factor appears, including the free energy gap between the charge storage state and P*. Consequently, the delayed fluorescence originating from Q_A-active RCs is more pronounced than that from Q_B-active RCs.

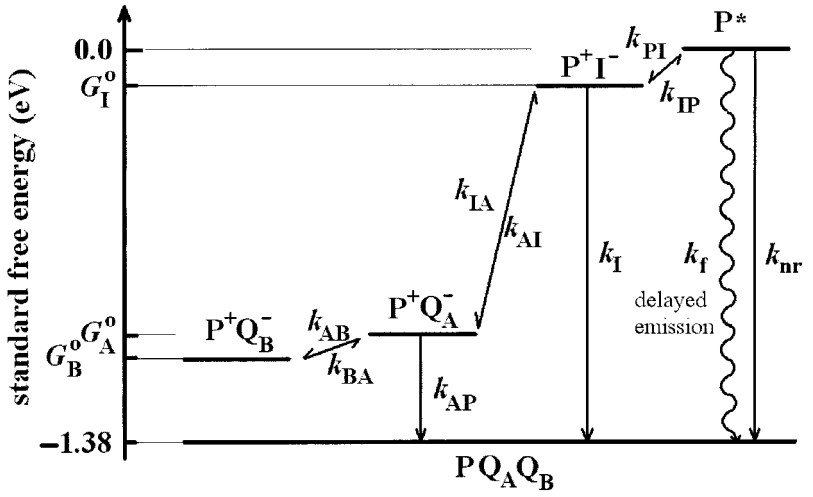

FIGURE 3 Origin of the leakage-type delayed fluorescence in RC of photosynthetic bacteria and the free energy levels of the redox states P^+I^-, $P^+Q_A^-$, $P^+Q_B^-$, and PQ_AQ_B relative to that of the excited state P*. The approximate rate constants of forward reactions are $k_{PI} = 3.6 \times 10^{11}\ s^{-1}$, $k_{IA} = 5.0 \times 10^9\ s^{-1}$, and $k_{AB} = 1.0 \times 10^4\ s^{-1}$. Note that there is no direct recombination from charge-separated state $P^+Q_B^-$.

RESULTS AND DISCUSSION

Immediately after the charge separation, the RC begins to emit delayed fluorescence in a very wide time domain. The decay consists of several phases indicating the contributions of more than one transient state in charge stabilization. The very fast (pico- and nanosecond) components reflect early reactions between high free energy states having static heterogeneity (Woodbury and Allen, 1995; Ogrodnik et al., 1999) and/or a time-dependent decrease (protein relaxation) (Woodbury and Parson, 1984; Peloquin et al., 1994; Woodbury et al., 1994) in their free energy levels. The study of these processes is beyond the scope of the present work. The sources of the slower (millisecond and second) components are lower-lying transient states, including the acceptor quinone complex that plays a central role in conservation of the photon energy. Depending on the redox state and reconstitution of the acceptor quinone complex, three different phases appear in the decay of the delayed fluorescence: a fastest, a fast, and a slow component with lifetimes (at pH 8.0) of 1.5 ms, 102 ms, and 865 ms, respectively (Fig. 4). These components can be attributed to different reactions in the RC and will be discussed separately below.

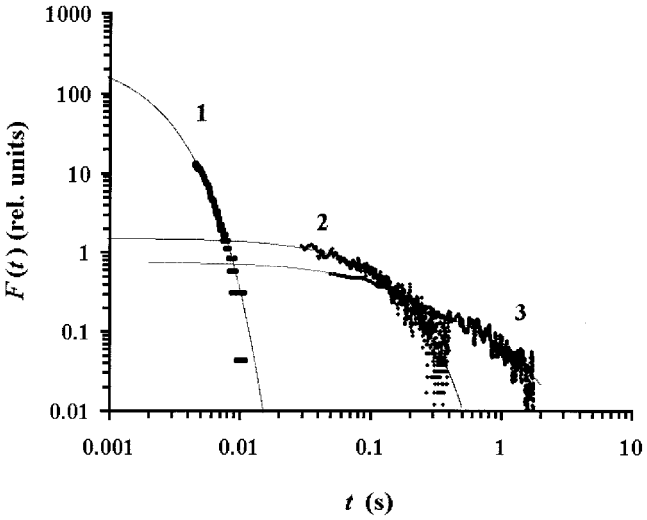

FIGURE 4 Kinetic traces of millisecond delayed fluorescence from bacterial RC in different states on a double logarithm scale. *Trace 1:* RC with photochemically reduced Q_A (pH 7.8). P^+ was rereduced by external donor ferrocene (10 μM) with a half-time of 10 ms as monitored by transient absorption change at 430 nm. The flash repetition rate was 2 Hz; other details are in the text. *Trace 2:* RC with oxidized primary quinone but secondary quinone activity blocked by terbutryne (100 μM, pH 8.0). *Trace 3:* RC with fully reconstituted secondary quinone activity (60 μM UQ_{10}, pH 8.2). The shutter is closed during the laser flash but is opened (*Trace 1:* within 3 ms) afterward. The time constants of the electronics were adjusted to the lifetimes of the components. Solid lines are the best fit for the sum of exponential functions with amplitudes and (lifetimes) of 310 (1.46 ms) (*Trace 1*), 1.52 (102 ms) (*Trace 2*), and 0.54 (115 ms) and 0.21 (865 ms) (*Trace 3*). Conditions: 1.3 μM RC, 0.03% TX-100, 10 mM Tris, and 100 mM NaCl.

Fastest component: BChl triplet-related process

To date, millisecond delayed fluorescence has been measured only at times longer than ~30 ms, probably because of limitations in shutter opening times (Arata and Parson, 1981; McPherson et al., 1990; Turzó et al., 1998). Using an order-of-magnitude shorter dead time, we could detect a previously neglected delayed fluorescence component with a lifetime in the range of several milliseconds (Fig. 4, *curve 1*). Unfortunately, the lifetime of the fastest phase could not be resolved with higher accuracy because of the overlapping shutter opening time.

Based on the following simple observations, we excluded the possibility that electrical artifacts could have significantly contributed to this fastest millisecond component. At the moment of the laser flash no signal was observed, although the detector was set at its highest sensitivity (only the shutter was closed). When the opening of the shutter was delayed relative to the laser flash, different parts of the same decay curve were measured.

The fastest component could arise from (very weak) phosphorescence (or delayed fluorescence) of the optical parts (cuvette, green filter, etc.) excited directly by the laser light or indirectly by the scattered light. These disturbing effects were carefully reduced by selection of a low-fluorescence cuvette and by placing the crucial optical elements in the emission path (red filter and lens) behind the shutter (Fig. 1). Blank solution (without RC) in the cuvette gave more than an order of magnitude smaller signal (artifact) than that with RC, even under the worst conditions.

Because of the very small intensity of the delayed light, its spectrum could not be resolved by inserting a monochromator in the fluorescence light path. However, when the high-pass filter (>850 nm) was replaced with an interference filter (λ_{max} = 919 nm, $\Delta\lambda$ = 20 nm, and T_{max} = 67%), the same properties of the delayed light (number, relative amplitudes, and life-times of the components) were measured.

Experiments using chemically and photochemically prereduced or preoxidized RCs offered the strongest arguments in favor of photochemical origin of the observed fastest component. No delayed fluorescence was measured at all when the dimer of the RC was preoxidized chemically by K-ferricyanide before the flash. This proves that the fastest component originates from the charge-separated state of the RC. When, however, the primary quinone in the RC was prereduced chemically by sodium dithionite before the laser light, the amplitude of the fastest component increased by more than one order of magnitude, while the fast component disappeared. Similar results were obtained when Q_A was prereduced photochemically (Fig. 4, *trace 1*). To keep Q_A in a reduced state, an external electron donor was added to the solution. Ferrocene was the best candidate for that purpose, as its fluorescence does not interfere with that of the RC and it is a relatively slow electron donor to P^+ (Maróti and Wraight, 1988). The experimental conditions

could be adjusted to optimally study the P^+X^- precursor state of the fastest component of delayed fluorescence. The rate of donation ($\sim 100\ s^{-1}$) was higher than that of the $P^+Q_A^- \rightarrow PQ_A$ charge recombination ($\sim 10\ s^{-1}$); thus the stable PQ_A^- redox state could accumulate but was much lower than the rate of $P^+I^- \rightarrow PI$ charge recombination ($k_I = 6 \times 10^7\ s^{-1}$) and the rate of disappearance of the P^+X^- precursor state ($\sim 10^3\ s^{-1}$) monitored by the fastest component of the delayed fluorescence.

The approximate free energy level of the P^+X^- precursor state of the fastest component was estimated from the plot of the logarithm of the amplitude as a function of reciprocal temperature (Fig. 5). The elevating temperature increases the extent of thermal repopulation of P* from P^+X^-, and therefore the intensity of the delayed fluorescence should increase (see Eq. 19 and the similar (van't Hoff) analysis for the fast and slow components). The low slope of the straight line in the van't Hoff plot ($\Delta H^\circ = -112$ meV) indicates that the P^+X^- precursor state has a high enthalpy relative to that of P*.

Evidently, additional experiments are required to describe the origin and characteristics of the fastest component of the millisecond delayed light, but several observations can be explained by using standard reaction paths of the RC (Fig. 3). In RC with reduced primary quinone, a transient charge separation between P and I takes place ($P \rightarrow P^* \rightarrow P^+I^-$), but instead of further stabilization of this charge pair by the primary quinone, parallel mechanisms (radical pair mechanism) and reaction paths to triplet formation ($^3(P^+I^-)$ and ^3P) become important (for a review see Volk et al., 1995). This is due to the increase in the lifetime of the P^+I^- state from 200 ps (when Q_A is oxidized) to ~15 ns (when Q_A is reduced). The higher amplitude of the fastest component of the delayed fluorescence observed upon prereduction of the primary quinone indicates that the precursor state should be filled *via* the transient P^+I^- state, and we argue that it should be related to either of the above-mentioned triplet states. The lifetime of the dimer triplet measured by electric and magnetic methods is 54 μs at room temperature (Volk et al., 1995), much shorter than the lifetime of the fastest component in the delayed fluorescence (~2 ms). It has been widely demonstrated, however, that static heterogeneity and/or relaxation processes may result in a diverse energetic landscape of the protein (Peloquin et al., 1994; Woodbury and Allen, 1995; Volk et al., 1995; Ogrodnik et al., 1999; Turzó et al., 1999). These effects, together with side reactions of the radical pair mechanism, may result in long-lived bacteriochlorophyll triplet states that may be difficult to trace in transient absorption because of their very low concentration and the lack of spectral distinction. The delayed fluorescence from these states, however, will be comparable to that originating from quinone levels (for quantitative analysis see Eq. 22).

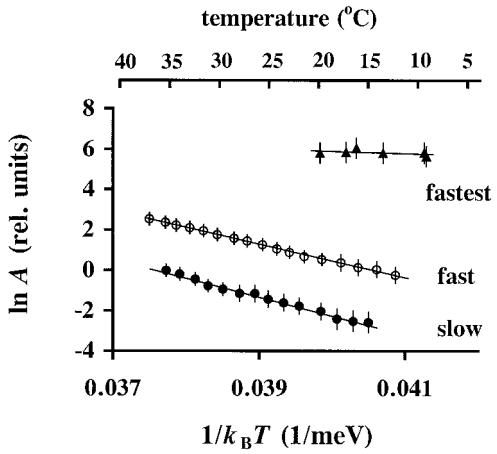

FIGURE 5 Van't Hoff plots of the amplitudes (A) of the different components of the millisecond delayed fluorescence (see Fig. 4) on the physiological temperature range. The enthalpy changes calculated from the slopes are −112 meV (▲, fastest phase), −828 meV (○, fast phase), and −932 meV (●, slow phase). The conditions are the same as in Fig. 4.

The quantum yield of the fastest component of the delayed fluorescence was determined by comparing the integrated light intensities of the prompt and delayed emissions. For the yield of the prompt fluorescence a value of 4×10^{-4} was taken (Zankel et al., 1968), which is in reasonable agreement with other recent measurements: 3.2×10^{-4} (Woodbury et al., 1985) and 1.2×10^{-4} (Nowak et al., 1998). Using this value together with the observed attenuation, a yield of 6.4×10^{-9} was obtained for the fastest component of the delayed fluorescence at pH 8.0.

Fast component: Q_A-related events

Evidence has accumulated in favor of the $P^+Q_A^-$ redox state of the RC as a precursor of the fast phase of the delayed fluorescence. If Q_A is prereduced chemically before the flash, this component is absent (Fig. 4, *curve 2*). The rate constant of the fast phase equals that of the transient absorption change reflecting the decay of the $P^+Q_A^-$ charge pair by recombination (Arata and Parson, 1981; Turzó et al., 1998). The slope of the van't Hoff plot of the fast component in the physiological temperature range yields a large enthalpy change (Fig. 5) that is characteristic of the charge stabilization on the primary quinone and makes the photochemical transition practically irreversible. The quantum yield of the fast component was found (as above) to be 2.2×10^{-9}.

The fast component has been proved to be sensitive to the chemical nature of the primary quinone (substitution), its protein environment (mutations), and the physicochemical properties of the bulk solution. Here the effect of pH and high-potential quinone substitution on the fast phase of the delayed fluorescence will be elaborated on in more detail.

Stabilization of $P^+Q_A^-$ by proton uptake of the RC

Based on Eq. 17, the free energy of the $P^+Q_A^-$ state relative to that of P* can be determined by measuring the ratio of the intensities of the prompt and delayed emissions (Arata and Parson, 1981). The amplitude of the fast component of the delayed light is extremely small: $A_{delay}/A_{prompt} = 2.3 \times 10^{-16}$ (4.4×10^{-15}; Arata and Parson, 1981), which indicates a considerable drop in the free energy of $P^+Q_A^-$ amounting to $G_A^\circ = -910 \pm 20$ meV (-860 ± 20 meV; Arata and Parson, 1981) at pH 7.8. The reason for the discrepancy between the two measurements is unknown. A rational possibility, the overestimation of the prompt fluorescence due to free pigments in our RC preparation, can be excluded. Within the precision of our experiments, we found that the excitation intensity dependence of the prompt fluorescence and that of the delayed fluorescence had similar saturations (data not shown). If the sample had contained free (or functionally decoupled) pigments with a much faster turnover rate ($\approx 1 \times 10^9$ s^{-1}) than the photochemistry of the RC (~ 10 s^{-1}), then their emission would have been expected to remain linear over many orders of magnitude of the excitation intensity before reaching saturation at much higher intensities than that for delayed fluorescence. Therefore, the fluorescence of the RC was not spoiled by extraneous emission.

The external H^+ ion concentration of the solution influences the free energy level of the $P^+Q_A^-$ charge pair, demonstrating the role of protonatable side chains of the protein in the interaction with the light-induced redox/charge state of Q_A (Maróti and Wraight, 1988). G_A° shows a marked drop in the alkaline pH range but becomes independent of pH below pH 7. The delayed fluorescence measurements for determination of the free energy of $P^+Q_A^-$ were extended to acidic pH values as low as pH 4. The observed pH dependence of the $P^+Q_A^-$ state is in good accordance with earlier measurements from Kleinfeld et al. (1985) and Sebban (1988), who assayed this state in the neutral and alkaline pH range, using a thermal back-reaction in RCs, in which the native ubiquinone was replaced with low-potential quinones (anthraquinones). Studies on site-directed mutant RCs have identified several protonatable residues in or near the Q_B binding pocket that interact with Q_A^- (Maróti et al., 1995; Miksovska et al., 1996; Kálmán et al., 1998) or with Q_B^- (Takahashi and Wraight, 1994; Okamura and Feher, 1995; Sebban et al., 1995). The cluster around Glu L212 in the Q_B binding domain is particularly responsive to Q_A^-, as demonstrated by the change in the free energy of $P^+Q_A^-$ in the alkaline pH range (UQ in Fig. 6). Above pH 8, G_A° drops by ~ 50 meV upon proton uptake of the Glu L212 cluster. This observation is a safe indication of the functional linkage between the Q_A and Q_B sites (Wraight, 1998). The type and path of interaction have not been clarified yet, as the distance of "cross-talk" is very large (~ 17 Å), and therefore interactions other than electrostatics should play an important role. The iron-histidine complex seems to be a proper

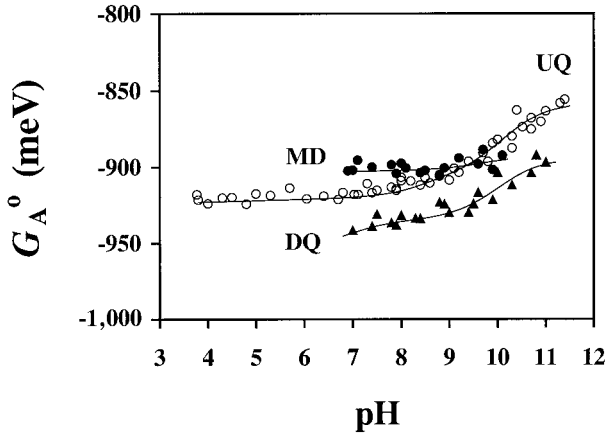

FIGURE 6 pH dependence of the free energy of $P^+Q_A^-$ relative to that of the excited dimer P*, determined by comparing the intensities of the prompt and delayed fluorescence. The primary quinone is either the native quinone (ubiquinone, UQ (○)) or an artificially substituted quinone analog (menadione, MD (●) or duroquinone, DQ (▲)). The secondary quinone binding site is occupied by 100 μM terbutryne, an effective interquinone electron transfer inhibitor. The solid lines represent the integrated proton uptake calculated from Henderson-Hasselbalch-type titration curves (see, *e.g.,* Turzó et al., 1999), with the following sets of pKs and shifts (ΔpK) of the individual protonatable amino acids. UQ: 4.87 (0.03), 6.87 (0.03), 8.35 (0.25), and 9.7 (0.8); DQ: 6.8 (0.3), 8.85 (0.05), and 9.7 (0.65); MD: 7.8 (0.02) and 9.6 (0.15).

wire along which coupling between the two quinone binding sites may be performed. Below pH 7, G_A° is pH independent, *i.e.,* other (acidic) clusters in the Q_B pocket or in the Q_A binding domain are not sensitive to the redox state of Q_A.

If the native ubiquinone is replaced by other quinones, the functional linkage can be perturbed. Substitution by DQ will not cause dramatic changes in the pH dependence of the free energy (only a small shift of about -20 meV), but replacement with MD almost completely eliminates the marked changes in the alkaline pH range (Maróti et al., 2000). Similar conclusion can be drawn from earlier flash-induced proton binding measurements in which no proton uptake was observed above pH 9 (Kálmán and Maróti, 1994). In trying to rationalize this peculiar pH behavior, we have to keep in mind that the white crystals of MD (2-methyl-1,4-naphthoquinone sodium bisulfite) are water soluble, which is unique among the quinone derivatives. During the process of substitution (when the Q_A pocket should be uncovered by a relatively large concentration of ionic detergent LDAO), some water molecules (together with the water-soluble MD) may invade the Q_A binding domain and can modify its dielectric property in a way that it screens the long-range electrostatic interactions. We argue that the electrostatic interaction between Q_A^- and the ionized Glu L212 near Q_B is attenuated by the increased effective dielectric constant, and therefore no pH changes in the alkaline pH range can be expected in the free energy level of $P^+Q_A^-$. An alternative explanation emphasizes the change in mobility of the protein environment upon substitution of UQ by MD.

The increased mobility involves a higher dielectric constant and thus reduced interaction between the charged groups in the two quinone binding pockets. These explanations need further proof from (molecular dynamic and/or electrostatic) calculations and experiments on different site-directed mutants and RCs where the native quinones are replaced by a wide variety of quinone analogs.

Free energy dependence of the rate of direct charge recombination from $P^+Q_A^-$

Much work has been devoted to investigating the effects of changes in G_A° on the ET properties of the RC (Gunner et al., 1986; Gunner and Dutton, 1989; McComb et al., 1990; Schelvis et al., 1992). The native Q_A was replaced by a variety of quinones differing in redox potential, and the delayed fluorescence of the substituted RC was measured relative to that of the RC with native ubiquinone (Woodbury et al., 1986). Based on the pioneering work of Woodbury et al. (1986), Gunner and Dutton (1989) found an empirical relationship between the free energy of the quinone (G_Q°) relative to that of the native ubiquinone (G_{UQ}°) and the charge recombination rate k_{AP} at pH 7.3 for a mechanism in which the back-reaction proceeds through thermal equilibration with the intermediate $P^+Q_A^-$:

$$G_Q^\circ - G_{UQ}^\circ = 56.6\ \text{meV} \cdot \log(k_{AP} - 7.0\ \text{s}^{-1}) + 53.1\ \text{meV} \quad (23)$$

The relationship predicts a 56.6-meV change in the $P^+Q_A^-$ level for a change in the rate of charge recombination by a factor of 10. Equation 23 is widely used to obtain estimates of the relative *in situ* redox potential for quinones with low potential (Graige et al., 1996; Schmid and Labahn, 1998).

The delayed fluorescence data of the present and related recent studies merit revisiting this subject for high-potential quinones at the Q_A binding site. As the conditions for Eq. 23 are not satisfied, changes in the expression should be considered. The $P^+Q_A^- \rightarrow PQ_A$ back-reaction occurs directly (by a tunneling mechanism) and indirectly via an uphill reaction through the thermally excited P^+I^- state, depending on the free energy of $P^+Q_A^-$ (see Fig. 3). Woodbury et al. (1986) estimated that the direct path dominates if $G_A^\circ < -800$ meV. The charge recombination rates for different high-potential (benzo- and naphtho)quinones at the Q_A binding site are plotted in Fig. 7 as the function of free energy of $P^+Q_A^-$ determined from delayed fluorescence measurements. All of these substituted RCs satisfied the above condition for a direct (temperature-independent) path of back-reaction. Three curves were fitted to the data. Curve G, calculated from the empirical relation (Eq. 23), is obviously not a good approximation ($\chi^2 = 20.83$) in this free energy range and should offer a better fit for low-potential quinones. Curve M, calculated from the commonly accepted Marcus theory of electron transfer in the high temperature limit,

$$k_{AP} = k_{max} \cdot \exp\left(- \frac{(- G_A^\circ - 1380\ \text{meV} + \lambda)^2}{4\lambda k_B T} \right) \quad (24)$$

gives a better result ($\chi^2 = 10.89$) with the two fitted parameters of the maximum rate constant $k_{max} = 50\ \text{s}^{-1}$ and reorganization energy $\lambda = 850$ meV. As the selected range of free energy is far away from the value where the rate reaches its maximum (-530 meV), the curvature is small and thus the fit is not very sensitive to the changes of the parameters. Even then, the fitted values are close to other

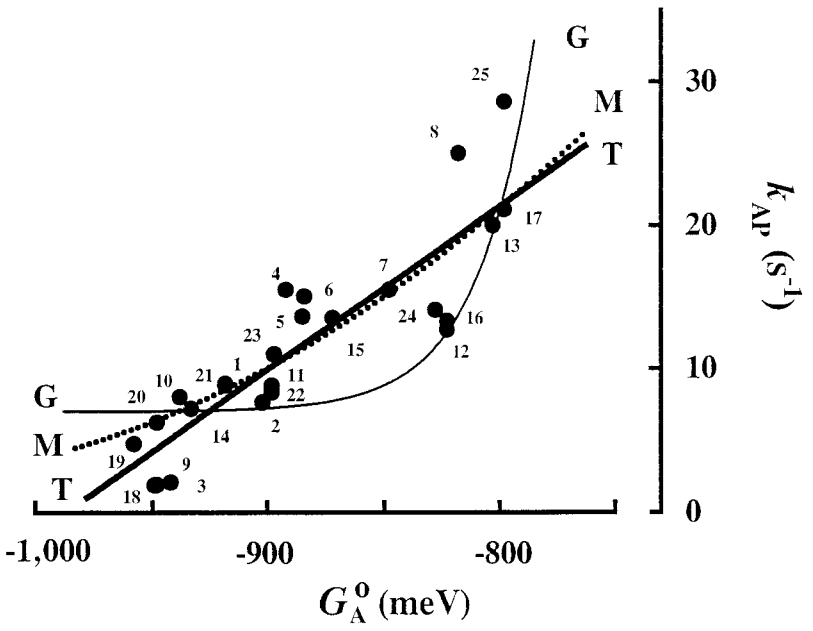

FIGURE 7 The observed rate constant of the $P^+Q_A^- \rightarrow PQ_A$ charge recombination (k_{AP}) as a function of the standard free energy of Q_A relative to that of the excited dimer (G_A°) for several "high potential" quinones at pH 7. *Samples 1–3:* UQ_{10}, MD, and DQ (this work); samples 4–8: 2-diisoprenyl-1,4-NQ (NQ_2), 2-methyl-1,4-NQ (MQ_0), 2-tetraisoprenyl-1,4-NQ (NQ_4), 2,3,5-trimethyl-1,4-NQ (TMNQ), and 2,3,6,7-tetramethyl-1,4-NQ (TEMNQ) (Li et al., unpublished results); *samples 9–13:* 1,4-benzoquinone tetramethyl, 1,4-NQ, 1,4-NQ 2,3-dimethyl, 1,4-NQ 2,3,5-trimethyl, and 1,4-NQ 5 methoxy (Gunner and Dutton, 1989); *samples 14–17:* MQ_0, 2-methyl-3-tetraisoprenyl-1,4-NQ (MQ_4), TMNQ and TEMNQ (Graige et al., 1996); samples 18–25: DQ, 6,7-dichloro NQ, 2-methylthio NQ, UQ, 2,3-dimethyl NQ, 5-methyl NQ, 2,3,5-trimethyl NQ, and 5-methoxy NQ (Woodbury et al., 1986). For the different sets of (mainly relative) measurements, $G_{UQ}^\circ = -918$ meV was taken. Fitted curves: T, fit of the straight line to the data (*thick line*) (standard $\chi^2 = 9.90$); M, Marcus expression (Eq. 24 with $k_{max} = 50\ \text{s}^{-1}$ and $\lambda = 850$ meV, *dotted line,* $\chi^2 = 10.89$); G, Gunner expression (Eq. 23, *thin line*, $\chi^2 = 20.83$, Gunner and Dutton, 1989).

estimates based on measurements using an external electric field (Feher et al., 1988) or mutants (Allen et al., 1998). The fit of the straight line to the data (T) gives the smallest χ^2 ($= 9.90$) value:

$$G_A^\circ = -987\text{meV} + 8.77\text{meV} \cdot s \cdot k_{AP} \qquad (25)$$

This is an empirical relationship between the rate of direct charge recombination and the free energy level of the primary quinone. Based on this expression, one can determine the *in situ* free energy of the $P^+Q_A^-$ state by measuring the rate of back-reaction in RCs where the native quinone is replaced by a high potential quinone.

Equation 25 indicates that the rate of direct recombination is only weakly dependent on the free energy of the primary quinone. The tunneling rate increases by 6.8 s^{-1} for every 60-meV increase in the free energy of the $P^+Q_A^-$ state. In contrast to this, the rate of the temperature-activated indirect path increases by a factor of 10 for each increase in the free energy of the $P^+Q_A^-$ state by 60 meV at room temperature (see Eq. 23).

Slow component: Q_B-associated events

If the secondary quinone activity of the RC is reconstituted, a long-lived delayed fluorescence can be observed (Arata and Parson, 1981; Fig. 4, *curve 3*). The lifetime corresponds to the lifetime of the $P^+Q_B^-$ state controlled by the indirect charge recombination via $P^+Q_A^-$ and can be as high as 1046 ms at pH 6.5. The quantum yield of the slow component was 2.6×10^{-9}. The free energy level of the precursor $P^+Q_B^-$ state relative to that of $P^+Q_A^-$ can be determined from the measured rates of the slow (k_{BP}) and fast (k_{AP}) components (Wraight and Stein, 1983; Kleinfeld et al., 1984):

$$G_B^\circ = G_A^\circ - k_B T \cdot \ln\left(\frac{k_{AP}}{k_{BP}} - 1\right) \qquad (26)$$

or from their amplitudes (Eq. 22). Whereas the former assay is widely applied (the rates can be determined with high precision from transient absorption measurements), the latter method shows one of the curiosities of the delayed fluorescence method. The pH dependence of the relevant quantities and a comparison of the free energy values provided by these two methods are shown in Fig. 8 for native RCs. The rates (Fig. 8, *top*) and the amplitudes (Fig. 8, *middle*) were determined from biexponential decomposition of the kinetics, and k_{AP} was measured in RCs with the secondary quinone removed. The rate of the fast component showed very weak pH dependence, but the rate of the slow phase exhibited a characteristic increase in the alkaline pH range in good accordance with earlier data (Kleinfeld et al., 1984). The relative amplitude of the slow phase of the transient absorption (S_{abs}) was high at neutral pH (>90%) but dropped with an increase in pH. Under our conditions, high pH did not favor the secondary quinone activity: either

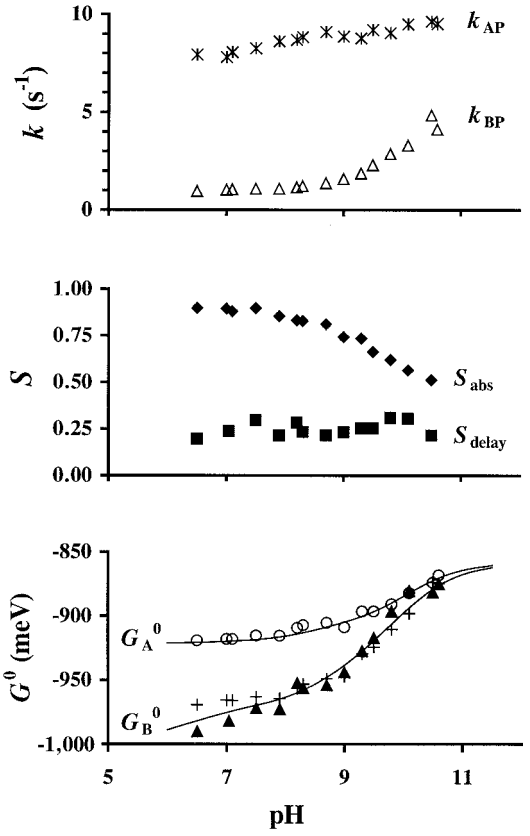

FIGURE 8 pH dependence of the free energy of $P^+Q_B^-$ in native RCs as determined from both the rate constants and the relative amplitudes of the slow phase of delayed fluorescence. (*Top*) Rate constants of charge recombination of RC with removed (k_{AP} (*)) and with reconstituted (k_{BP} (△)) secondary quinone activity determined from transient absorption data. These are the same rate constants as those of the corresponding delayed fluorescence decay, but they can be determined more accurately. (*Middle*) Relative amplitudes of the slow component of transient absorption (S_{abs}, ◆) and delayed fluorescence (S_{delay}, ■), as calculated using Eqs. 20 and 21, respectively. (*Bottom*) Free energies of $P^+Q_B^-$, as determined using Eqs. 26 (+) and 22 (▲) and the free energy level of $P^+Q_A^-$ (○) (see Fig. 6).

the apparent quinone affinity or the availability of quinones to the secondary quinone binding site from the pool decreased. The relative amplitude of the slow phase of the delayed fluorescence (S_{delay}) was low (~25%) and remained constant in our pH range. This is in accordance with the expectation that the contribution of precursors to the observed delayed fluorescence is not according to their concentrations but is further weighted by their free energy levels. The free energy of $P^+Q_B^-$ can be derived from both the kinetic rate constants and the fractional amplitude of the slow phase, using Eqs. 26 and 22, respectively. These two (kinetic and delayed fluorescence) methods are almost consistent, as they offer similar results within the precision of the measurements (Fig. 8, *bottom*).

The pH dependence of G_B° is more complex and more profound than that of G_A°, indicating that more protonatable residues are responding to Q_B^- formation and they are closer

to the secondary semiquinone. This is not surprising, as many more ionizable groups are in or around the Q_B binding pocket than in the Q_A binding site. Recent calculations on protein and proton motions upon interquinone electron transfer revealed that a cluster of acids near Q_B (Glu L212, Asp L213, and Asp L210) could play a crucial role in the determination of the pH profile of the free energy of the P^+Q^- charge-separated state (Alexov and Gunner, 1999). The observed difference in the low pH behavior of the $P^+Q_A^-$ and $P^+Q_B^-$ states can be attributed to the difference in charge distribution of the cluster. In the $P^+Q_B^-$ state, the negative charge of the cluster is shifted to the more distant Asp L210, and its interaction with Q_B^- describes the observed stabilization of the $P^+Q_B^-$ state in the acidic pH range.

CONCLUSIONS

Because of its leakage type, the delayed fluorescence from isolated photosynthetic reaction center protein is an excellent probe of intraprotein electron transfer, as it monitors but does not influence the primary processes. The extremely low quantum yield of millisecond delayed fluorescence calls for a sophisticated optical and electronic arrangement not readily available for routine assays. Comparative delayed fluorescence, transient absorption, and theoretical studies revealed a number of interesting kinetic and thermodynamic aspects of charge stabilization after flash excitation. The three distinct phases in the millisecond delayed fluorescence account for different steps in the stabilization of the primary charge pair. By measuring the ratio of the prompt and delayed fluorescence intensities, one can determine the free energy level of the precursor state relative to the free energy level of the excited dimer that is not exposed to direct influences of the cytoplasmic side of the RC. This allows the determination of the *in situ* positions of the different quinone states on the free energy scale. The delayed fluorescence is sensitive even to slight changes in the free energy level due to proton uptake or quinone substitution. The functional linkage between the two quinone binding sites was demonstrated by measuring the interaction energy between the primary semiquinone and the protonatable Glu L212 cluster in the Q_B pocket. Based on a series of delayed fluorescence data on high potential quinones, an empirical expression was found. This calibration straight line makes it possible to estimate the free energy of the primary charge pair from the measured rate constant of direct charge recombination, i.e., from an easily available kinetic parameter.

We thank Dr. L. Nagy and Mr. L. Gerencsér for helpful discussions.

This work was supported by grants from the Hungarian Science Foundation (OTKA T30337 and M27903), the Foundation of the Hungarian Ministry of Education (FKFP 1288 and B-23/1997, FEFA III/1034 and IV/1605, PFP 1999/0422 and AMFK 043/98), the Hungarian and French governments (Balaton 2000-02), and NATO (LST.CLG 975754).

REFERENCES

Alexov, E. G., and M. R. Gunner. 1999. Calculated protein and proton motions coupled to electron transfer: electron transfer from Q_A^- to Q_B in bacterial photosynthetic reaction centers. *Biochemistry.* 38:8253–8270.

Allen, J. P., J. C. Williams, M. S. Graige, M. L. Paddock, A. Labahn, G. Feher, and M. Y. Okamura. 1998. Free energy dependence of the direct charge recombination from the primary and secondary quinones in reaction centers from *Rhodobacter sphaeroides. Photosynth. Res.* 55: 227–233.

Arata, H., and W. W. Parson. 1981. Delayed fluorescence from *Rhodopseudomonas sphaeroides* reaction centers. Enthalpy and free energy changes accompanying electron transfer from P-870 to quinones. *Biochim. Biophys. Acta.* 638:201–209.

Arlt, T., S. Schmidt, W. Kaiser, C. Lauterwasser, M. Meyer, H. Scheer, and W. Zinth. 1993. The accessory bacteriochlorophyll: a real electron carrier in primary photosynthesis. *Proc. Natl. Acad. Sci. USA.* 90: 11757–11761.

Cramer, W. A., and D. B. Knaff. 1990. Energy Transduction in Biological Membranes. Springer-Verlag, New York, Berlin, and Heidelberg.

Feher, G., T. R. Arno, and M. Y. Okamura. 1988. The effect of an electric field on the charge recombination rate of $D^+Q_A^- \rightarrow DQ_A$ in reaction centers from *Rhodobacter sphaeroides* R-26. *In* The Photosynthetic Bacterial Reaction Center. J. Breton and A. Vermeglio, editors. Plenum Press, New York. 271–287.

Fleischman, D. 1978. Delayed fluorescence and chemiluminescence. *In* The Photosynthetic Bacteria. R. K. Clayton and W. R. Sistrom, editors. Plenum Press, New York. 513–523.

Fleming, G. R., J.-L. Martin, and J. Breton. 1988. Rates of primary electron transfer in photosynthetic reaction centers and their mechanistic implications. *Nature.* 333:190–192.

Graige, M. S., M. L. Paddock, J. M. Bruce, G. Feher, and M. Y. Okamura. 1996. Mechanism of proton-coupled electron transfer for quinone (Q_B) reduction in reaction centers of *Rb. sphaeroides. J. Am. Chem. Soc.* 118:9005–9016.

Gunner, M. R., and P. L. Dutton. 1989. Temperature and $-\Delta G°$ dependence of the electron transfer from $BPh^{\bullet -}$ to Q_A in reaction center protein from *Rhodobacter sphaeroides* with different quinones as Q_A. *J. Am. Chem. Soc.* 111:3400–3412.

Gunner, M. R., D. E. Robertson, and P. L. Dutton. 1986. Kinetics study on the reaction center protein from *Rhodopseudomonas sphaeroides:* the temperature and free energy dependence of electron transfer between various quinones in the Q_A site and the oxidized bacteriochlorophyll dimer. *J. Phys. Chem.* 90:3783–3795.

Kálmán, L., and P. Maróti. 1994. Stabilization of reduced primary quinone by proton uptake in reaction centers of *Rhodobacter sphaeroides. Biochemistry.* 33:9237–9244.

Kálmán, L., P. Sebban, D. K. Hanson, M. Schiffer, and P. Maróti. 1998. Flash-induced changes in buffering capacity of reaction centers from photosynthetic bacteria reveal complex interaction between quinone pockets. *Biochim. Biophys. Acta.* 1365:513–521.

Kleinfeld, D., M. Y. Okamura, and G. Feher. 1984. Electron transfer in reaction centers of *Rhodopseudomonas sphaeroides.* 1. Determination of the charge recombination pathway of $D^+Q_AQ_B^-$ and free energy and kinetic relations between $Q_A^-Q_B$ and $Q_AQ_B^-$. *Biochim. Biophys. Acta.* 766:126–140.

Kleinfeld, D., M. Y. Okamura, and G. Feher. 1985. Charge recombination kinetics as a probe of protonation of the primary acceptor in photosynthetic reaction centers. *Biophys. J.* 48:849–852.

Labahn, A., M. L. Paddock, P. H. McPherson, M. Y. Okamura, and G. Feher. 1994. Direct charge recombination from $D^+Q_AQ_B^-$ to DQ_AQ_B in bacterial reaction centers from *Rhodobacter sphaeroides. J. Phys. Chem.* 98:3417–3423.

Li, J., D. Gilroy, D. M. Tiede, and M. R. Gunner. 1998. Kinetic phases in the electron transfer from $P^+Q_A^-Q_B$ to $P^+Q_AQ_B^-$ and the associated

processes in *Rhodobacter sphaeroides* R-26 reaction centers. *Biochemistry.* 37:2818–2829.

Liu, B.-L., L.-H. Yang, and A. J. Hoff. 1991. On the depletion and reconstitution of both Q_A and metal in reaction centers of the photosynthetic bacterium *Rb. sphaeroides* R-26. *Photosynth. Res.* 28:51–58.

Maróti, P., D. K. Hanson, M. Schiffer, and P. Sebban. 1995. Long-range electrostatic interaction in the bacterial photosynthetic reaction centre. *Nature Struct. Biol.* 2:1057–1059.

Maróti, P., K. Turzó, G. Laczkó, and Z. Filus. 2000. Quinone-dependent energetics of charge separated states of bacterial reaction center. *Biophys. J.* 78:338A.

Maróti, P., and C. A. Wraight. 1988. Flash-induced H^+ binding by bacterial photosynthetic reaction centers: comparison of spectrophotometric and conductimetric methods. *Biochim. Biophys. Acta.* 934:314–328.

Martin, J.-L., J. Breton, A. J. Hoff, A. Migus, and A. Antonetti. 1986. Femtosecond spectroscopy of electron transfer in the reaction center of the photosynthetic bacterium *Rhodospeudomonas sphaeroides* R-26: direct electron transfer from the dimeric bacteriochlorophyll primary donor to the bacteriopheophytin acceptor with time constant of 2.8 ± 0.2 psec. *Proc. Natl. Acad. Sci. USA.* 83:957–961.

McComb, J. C., R. R. Stein, and C. A. Wraight. 1990. Investigation on the influence of headgroup substitution and isoprene side-chain length in the function of primary and secondary quinones of bacterial reaction centers. *Biochim. Biophys. Acta.* 1015:156–171.

McPherson, P. H., V. Nagarajan, W. W. Parson, M. Y. Okamura, and G. Feher. 1990. pH dependence of the free energy gap between DQ_A and $D^+Q_A^-$ determined from delayed fluorescence in reaction centers from *Rhodobacter sphaeroides* R-26. *Biochim. Biophys. Acta.* 1019:91–94.

Miksovska, J., P. Maróti, J. Tandori, M. Schiffer, D. K. Hanson, and P. Sebban. 1996. Distant electrostatic interactions modulate the free energy level of Q_A^- in the photosynthetic reaction center. *Biochemistry.* 35: 15411–15417.

Nowak, F. R., J. T. M. Kennis, E. M. Franken, A. Ya. Shkuropatov, A. Yakovlev, P. Gast, A. J. Hoff, T. J. Aartsma, and V. A. Shuvalov. 1998. The energy level of $P^+B_A^-$ in plant pheophytin-exchanged bacterial reaction centers probed by the temperature dependence of delayed fluorescence. *In* Photosynthesis: Mechanisms and Effects, Vol. 2. G. Garab, editor. Kluwer Academic Publishers, Dordrecht, the Netherlands. 783–786.

Ogrodnik, A., G. Hartwich, H. Lossau, and M. E. Michel-Beyerle. 1999. Dispersive charge separation and conformational cooling of $P^+H_A^-$ in reaction centers of *Rb. sphaeroides* R26: a spontaneous emission study. *Chem. Phys.* 244:461–478.

Okamura, M. Y., and G. Feher. 1995. Proton-coupled electron transfer reactions of Q_B in reaction centers from photosynthetic bacteria. *In* Anoxygenic Photosynthetic Bacteria. R. E. Blankenship, M. T. Madigan, and C. E. Bauer, editors. Kluwer Academic Publishers, Dordrecht, Boston, and London. 577–594.

Okamura, M. Y., R. A. Isaacson, and G. Feher. 1975. Primary acceptor in bacterial photosynthesis: obligatory role of ubiquinone in photoactive reaction centers of *Rhodopseudomonas sphaeroides. Proc. Natl. Acad. Sci. USA.* 72:3491–3495.

Osváth, Sz., G. Laczkó, P. Sebban, and P. Maróti. 1996. Electron transfer in reaction centers of *Rhodobacter sphaeroides* and *Rhodobacter capsulatus* monitored by fluorescence of the bacteriochlorophyll dimer. *Photosynth. Res.* 47:41–49.

Osváth, SZ., and P. Maróti. 1997. Coupling of cytochrome and quinone turnovers in photocycle of reaction center from photosynthetic bacteria *Rhodobacter sphaeroides. Biophys. J.* 73:972–982.

Peloquin, J. M., J. C. Williams, X. Lin, R. G. Alden, A. K. W. Taguchi, J. P. Allen, and N. W. Woodbury. 1994. Time-dependent thermodynamics during early electron transfer in reaction centers from *Rhodobacter sphaeroides. Biochemistry.* 33:8089–8100.

Schelvis, J. P. M., B.-L. Liu, T. J. Aartsma, and A. J. Hoff. 1992. The electron transfer rate from BPh_A^- to Q_A in reaction centers of *Rhodobacter sphaeroides* R-26: influence of the H-subunit, the Q_A and Fe^{2+} cofactors, and the isoprene tail of Q_A. *Biochim. Biophys. Acta.* 1102:229–236.

Schmid, R., F. Goebel, A. Warnecke, and A. Labahn. 1999. Synthesis and redox potentials of methylated vitamin K derivatives. *J. Chem. Soc. Perkin Trans.* 2:1199–1202.

Schmid, R., and A. Labahn. 1998. The influence of quinone structure on quinone binding to the Q_A site in bacterial reaction centers from *Rhodobacter sphaeroides. In* Photosynthesis: Mechanisms and Effects, Vol. 2. G. Garab, editor. Kluwer Academic Publishers, Dordrecht, the Netherlands. 877–880.

Sebban, P. 1988. pH effect on the biphasicity of the $P^+Q_A^-$ charge recombination kinetics in the reaction centers from *Rhodobacter sphaeroides,* reconstituted with anthraquinones. *Biochim. Biophys. Acta.* 936: 124–132.

Sebban, P., P. Maróti, M. Schiffer, and D. K. Hanson. 1995. Electrostatic dominoes: long distance propagation of mutational effects in photosynthetic reaction centers of *Rhodobacter capsulatus. Biochemistry.* 34: 8390–8397.

Takahashi, E., and C. A. Wraight. 1994. Molecular genetic manipulation and characterization of mutant photosynthetic reaction centers from purple nonsulfur bacteria. *In* Advances in Molecular and Cell Biology, Vol. 10. JAI Press, Greenwich, CT. 197–251.

Turzó, K., G. Laczkó, and P. Maróti. 1998. Delayed fluorescence study on $P^*Q_A \rightarrow P^+Q_A^-$ charge separation energetics linked to protons and salt in reaction centers from *Rhodobacter sphaeroides. Photosynth. Res.* 55:235–240.

Turzó, K., G. Laczkó, and P. Maróti. 1999. Proton binding is part of protein relaxation of flash excited reaction center from photosynthetic bacteria *Rhodobacter sphaeroides. Isr. J. Chem.* 39:447–455.

Volk, M., A. Ogrodnik, and M.-E. Michel-Beyerle. 1995. The recombination dynamics of the radical pair P^+H^- in external magnetic and electric fields. *In* Anoxygenic Photosynthetic Bacteria. R. E. Blankenship, M. T. Madigan, and C. E. Bauer, editors. Kluwer Academic Publishers, Dordrecht, Boston, and London. 595–626.

Woodbury, N. W., and J. P. Allen. 1995. The pathway, kinetics and thermodynamics of electron transfer in wild type and mutant reaction centers of purple nonsulfur bacteria. *In* Anoxygenic Photosynthetic Bacteria. R. E. Blankenship, M. T. Madigan, and C. E. Bauer, editors. Kluwer Academic Publishers, Dordrecht, Boston, and London. 527–557.

Woodbury, N. W., M. Becker, D. Middendorf, and W. W. Parson. 1985. Picosecond kinetics of the initial photochemical electron transfer reaction in bacterial photosynthetic reaction centers. *Biochemistry.* 24: 7516–7521.

Woodbury, N. W., and W. W. Parson. 1984. Nanosecond fluorescence from isolated photosynthetic reaction centers of *Rhodopseudomonas sphaeroides. Biochim. Biophys. Acta.* 767:345–361.

Woodbury, N. W., W. W. Parson, M. R. Gunner, R. C. Prince, and P. L. Dutton. 1986. Radical-pair energetics and decay mechanisms in reaction centers containing anthraquinones, naphtoquinones or benzoquinones in place of ubiquinone. *Biochim. Biophys. Acta.* 851:6–22.

Woodbury, N. W., J. M. Peloquin, R. G. Alden, X. Lin, S. Lin, A. K. W. Taguchi, J. C. Williams, and J. P. Allen. 1994. Relationship between thermodynamics and mechanism during photoinduced charge separation in reaction centers from *Rhodobacter sphaeroides. Biochemistry.* 33: 8101–8112.

Wraight, C. A. 1998. Functional linkage between the Q_A and Q_B sites of photosynthetic reaction centers. *In* Photosynthesis: Mechanisms and Effects, Vol. 2. G. Garab, editor. Kluwer Academic Publishers, Dordrecht, the Netherlands. 693–698.

Wraight, C. A., and R. K. Clayton. 1973. The absolute quantum efficiency of bacteriochlorophyll photooxidation in reaction centers of *Rhodobacter sphaeroides. Biochim. Biophys. Acta.* 333:246–260.

Wraight, C. A., and R. R. Stein. 1983. Bacterial reaction centers as a model for photosystem II: turnover of the secondary acceptor quinone. *In* The Oxygen Evolving System of Photosynthesis. Y. Inoue, A. R. Crofts, Govindjee, N. Murata, G. Renger, and K. Satoh, editors. Academic Press, Tokyo, Orlando, and San Diego. 383–392.

Zankel, K. L., D. W. Reed, and R. K. Clayton. 1968. Fluorescence and photochemical quenching in photosynthetic reaction centers. *Proc. Natl. Acad. Sci. USA.* 61:1243–1249.